Numerical Modeling of Hydrodynamic Performance on Porous Slope Type Floating Breakwater

Numeričko modeliranje hidrodinamičke izvedbe na poroznom kosom tipu plutajućeg lukobrana

Sujantoko*
Institut Teknologi Sepuluh
Nopember (ITS)
Department of Ocean Engineering
Surabaya, Indonesia
E-mail: sujantoko@oe.its.ac.id

Wisnu Wardhana
Institut Teknologi Sepuluh
Nopember (ITS)
Department of Ocean Engineering
Surabaya, Indonesia
E-mail: wisnu@oe.its.ac.id

Eko Budi Djatmiko
Institut Teknologi Sepuluh
Nopember (ITS)
Department of Ocean Engineering
Surabaya, Indonesia
E-mail: ebdjatmiko@oe.its.ac.id

Is Naldi Gemilang Firmasyah
Institut Teknologi Sepuluh
Nopember (ITS)
Department of Ocean Engineering
Surabaya, Indonesia
E-mail: naldifirmansyah09@gmail.com

Abstract

A floating breakwater is a coastal building that aims to break up or withstand wave energy that enters the beach so that the characteristics of the incoming waves are by calculations and can reduce abrasion on the shoreline. Designing a floating breakwater is very complicated because it depends on many aspects. These fundamental aspects depend on each other, so if one of these aspects changes, the integrity of the floating breakwater structure will also change. One of these aspects is the magnitude of the transmission and reflection coefficients generated by the floating breakwater. This research will study the hydrodynamic performance of floating breakwater due to variations in slope and porosity in reducing and reflecting waves with computational fluid dynamics (CFD). The slope-porous floating breakwater dimension is based on previous experimental data, including a constant water depth of 0.75 m, a wave height of 0.05 - 0.125 m, and a wave period of 1.1 - 2 sec on regular waves. The results of the numerical model validation and experiments on all variations of the floating breakwater model are quite good, which is less than 10% for both wave transmission and reflection. Analysis of the influence of changes in the mooring line angle, the simulation is carried out at an angle of 30 deg to 90 deg and produces an average transmission coefficient of 0.79 and a reflection of 0.21. While the effect of changes in water level elevation (0.85 m, 0.75 m, and 0.65 m) gives a reasonably significant average transmission coefficient of 0.85 and a reflection of 0.13. The mooring line angle will be gentler at high tide, and the transmission and reflection coefficients will be higher. However, the mooring line will loosen at low tide, causing the structure to move more freely and eliminating the function of the floating breakwater itself so that the tidal phenomenon becomes a challenge for coastal experts in designing structures to produce effective and efficient hydrodynamic performance.

Sažetak

Lukobran je obalna građevina koja ima za cilj smanjiti ili odbaciti energiju valova koji dolaze na obalu. Karakteristike dolaznih valova izračunate su kalkulacijama i mogu smanjiti abraziju obale. Projektiranje plutajućega lukobrana vrlo je složeno jer ovisi o više aspekata. Ovi temeljni aspekti ovise jedni o drugima, stoga ako se jedan od aspekata mijenja, integritet strukture plutajućega lukobrana također se mijenja. Jedan je od ovih aspekata magnituda transmisije i koeficijenti refleksije koje generira plutajući lukobran. Ovo istraživanje proučavat će hidrodinamičku izvedbu plutajućega lukobrana zbog varijacija kosine i poroznosti pri smanjivanjj i reflektiranjj valova računalnim dinamičkim modelom (CFD). Dimenzija kosog poroznog plutajućeg lukobrana temelji se na prethodnim eksperimentalnim podacima, uključujući konstantnu dubinu vode od 0,75 m, visinu vala od 0,05 do 0,125 m i period vala od 1,1 do 2 sekunde na pravilnim valovima. Rezultati validacije numeričkoga modela i eksperimenti na svim varijacijama modela plutajućega lukobrana prilično su dobri, što je manje od 10% i za prijenos vala i za refleksiju. Analiza utjecaja promjena u kutu užeta za privezivanje napravljena je simulacijom pod kutom od 30 do 90 stupnjeva te proizvodi prosječni koeficijent transmisije od 0,79 i refleksiju od 0,21. Efekt promjena u razini podizanja vode (0,85 m, 0,75 m i 0,65 m) daje razumno značajan prosječni koeficijent transmisije od 0,85 i refleksiju od 0,13. Kut užeta za privezivanje bit će slabiji pri plimi, a transmisijski i refleksijski koeficijenti bit će viši. Međutim, uže za privezivanje olabaviti će se pri oseci, uzrokujući da se struktura giba što slobodnije i eliminira funkciju plutajućega lukobrana samoga, tako da fenomen morske mijene postaje izazov za obalne stručnjake pri dizajniranju struktura koje će ostvariti djelotvornu i učinkovitu hidrodinamičku izvedbu.

* Corresponding author

1. INTRODUCTION / *Uvod*

The propagation of waves to the coast can be diffraction, refraction, shoaling, transmission, and reflection processes that will affect changes in wave energy on the beach. Wave energy has a broad spectrum, so its comprehensive treatment is often complicated, and this is an exciting aspect for coastal engineers. Many coastlines experience coastal de-stabilization conditions due to erosion and sedimentation. These two factors will endanger the potential of coastal areas by disrupting coastal resources and wealth and economic activities in coastal areas, such as tourism, aquaculture, housing, mangroves, sandy beaches, infrastructure, ponds, and others [1-5]. In addition, the propagation of high waves can also affect the mooring of ships and loading and unloading activities at the port. Calm sea wave conditions are needed so that activities at the port can run smoothly.

Regional planning for coastal activities requires consideration of factors of natural conditions and the surrounding environment and other economic factors. So often, coastal activity areas are selected based on topographical conditions that can provide natural protection in planning, such as an island-protected beach. In some cases, wave protection with natural topography often does not meet the required protection demands, so an artificial coastal protection structure is needed that can absorb the waves [6]. The natural condition of the waves and the desired level of wave protection will determine the type and design of the breakwater, the dimensions, and the configuration required [7].

The rubble-mound or caisson-type breakwater offers the advantage of excellent wave energy damping and has been widely used [8-11]. However, this type of coastal protection becomes uneconomical for relatively steep and deep coastal waters and large waves because construction costs will increase drastically [12]. In addition, the average steep coast has rough and poor seabed conditions that affect the stability of the structure [13], as well as frequent changes in water flow circulation, which can cause erosion and sedimentation in the surrounding area [14].

Floating Breakwaters offer the protection needed when working in deeper waters with more vital natural forces than fixed breakwaters. The Structure uses the visions of reflection, dissipation, and transformation to dampen the wave energy to attenuate the incident wave [15]. Floating breakwaters provide primary or additional protection against waves where reefs, shallow seabeds, or conventional fixed structures support wave protection. These structures are generally installed in marinas, ports, tourist areas, and aquaculture facilities. Floating breakwater has several advantages [12, 15, 16], namely, it can be easily moved, and its layout can be rearranged because of its transportability and flexibility in design. It can be applied to soil conditions on the seabed with poor systems. Mooring ropes do not interfere with water circulation, sediment transport, and fish migration, low current circulation in conventional breakwaters will result in an accumulation of sediment concentration in the area, and construction time is relatively short. Floating breakwaters also offer a low and economical alternative to construction costs compared to conventional breakwaters, especially in water depths of more than 3.05m [17]. Apart from the primary function as a wave absorber, this structure can also function as a walkway, marine habitat, seawall, and ship dock.

In addition to the advantages of the floating breakwater, it also poses several disadvantages that require careful evaluation. The design and development of floating breakwaters for coastal areas is a significant challenge for engineering engineers. The structure design at the specified location should carefully consider wave height analysis. Some drawbacks include limitations for short fetch lengths, structure life (10-20 yrs), and part of the transmitted incident wave [16]. Hales [17] stated there was uncertainty about the magnitude and type applied to the system and the insufficiency of information on maintenance expenses. So being conservative in design practice will increase construction costs. The main disadvantage of floating breakwaters is that these structures always move in reaction to waves, making the system more easily fatigued.

Wave energy can be reduced by taking care of reflecting waves and destroying the motion of wave particles by floating breakwaters. Their reflectivity and interference depend on the structure's shape, dimensions, surface, and design configuration. Floating breakwaters can cause wave diffraction, i.e., waves coming from different directions will break apart when they hit the structure. In this process, the wave energy will be transformed into the motion energy of the structure. The greater the wave energy absorbed by the structure, the higher the intensity of the motion of the structure. The amount of energy absorbed depends on the cross-sectional area of the structure to the direction perpendicular to the wave. So that in the floating breakwater design, the minimum cross-section and the interaction effect become an essential reference to produce a floating breakwater with the slightest motion response [18]. The study of the shape of the porous structure is very beneficial because, in addition to being able to dampen waves, the wave energy received by the structure and the mooring line becomes small [19, 20].

This research studies a porous slope floating breakwater anchored in the sea. The pore shape of this structure aims to reduce the excessive wave load that impacts its performance. In the impermeable form, the structure will cause a maximum structural motion response, increasing the mooring line stress. Based on experimental results [21], researchers will examine the hydrodynamic performance of floating breakwater due to the influence of slope and porosity by computing fluid dynamics.

This study aims to determine the optimum floating breakwater performance by comparing the reflection and transmission coefficients based on experimental and numerical results. This paper is organized with the following steps: *Step 1* is numerical modeling (computational fluid dynamics) based on previous experimental data. *Step 2* analyzes and validates the transmission and reflection of the numerical model and experiment results. *Step 3* studies the effect of the mooring line angle and water level elevation. Steps 2 and 3 are included in the results and discussion, and *the last step* contains conclusions and suggestions from this research.

2. LITERATURE REVIEW / *Pregled literature*

Research on floating breakwaters was initially investigated by Nece and Richey [22]. Floating breakwaters objects are in the form of twin-hull pontoons and pontoon boxes. Along with industrial developments in structure module manufacturing, many floating breakwaters are chain-moored rectangular caissons with two vertical plates protruding downwards from the sides, such as the Π-type shape. Furthermore, various forms and configurations of floating breakwaters were investigated by several researchers. Blumberg and Cox [23] conducted experiments on flumes of various configurations (box, T-shape, and catamaran). Based on his research, the curve of transmission coefficient and maximum horizontal wave load was obtained. Neelamani and Rajendran [24, 25] focused on examining T-type and ⊥-type floating breakwaters. Transmission, reflection, and energy dissipation were experimentally tested on regular and random waves—the transmission coefficient decreases as the steepness of the waves and the relative water depth d/L increase. Two floating breakwaters are very efficient at reducing incident wave energy. T-type floating breakwater is better than ⊥-type by about 20-30%. Dong et al. [26] tested three types of floating breakwaters with a physical model: box shape, double box, and plank net. The results found that the board-net floating breakwater is a simple and cheap structure that can be applied to deep-water aquaculture. Koutados et al. [27] investigated four forms of floating breakwaters. In this study, it can be found that the efficiency of the floating breakwater will increase if the plate is installed in front of the structure.

In addition to experimental research, the behavior of floating breakwaters is also studied numerically. Several researchers, including Fuguzza and Natale [28], built a combined linear model, namely the movement of the structure and wave diffraction, to describe a floating breakwater in the form of a box on a regular wave. The results of the numerical model show conformity with the physical model test. Sannasiraj et al. [29] tested a 2-D numerical model to evaluate the coefficients and hydrodynamic forces on angular waves in a floating breakwater in the form of a pontoon. The 2-D model can be applied to study wave-structure interaction problems. Rahman et al. [30] verified the numerical model with experiments for rectangular floating breakwaters. The results represent water level elevation at different offshore and onshore locations and the dynamic displacement of the floating structure. The forces on the mooring line and the hydrodynamic coefficients are compared to the experimental results. Gesraha [31] proved numerical studies and experiments on the rectangular-type floating breakwater with two thin sideboards vertically downwards, Π-type. The results show that for the angular wave to the structure, the highest wave transmission occurs compared to the rectangular type.

The study of extreme loads that occur in the ocean on floating breakwaters has also been investigated by Cox et al. [32] tested the performance of the box type on regular and random waves, namely transmission, reflection, and dissipation of waves, motion, and structural stability due to wave forces. Ruol and Martinelli [33] tested various mooring lines on the floating breakwater type Π, chains with different initiating tension or pile. The analysis concentrated on mooring line forces, chain shock loads, and wave transmission. Furthermore, The performance of type Π floating breakwater in different incident wave directions was studied by Martinelli et al. [34]. The results of this test show that an increased wave incident angle will reduce wave transmission and mooring forces due to shock loads on the chain will also decrease, and the binding force will slightly increase.

In recent research, several researchers investigated the sensitivity of the floating breakwater transmission coefficient as a dimensionless parameter, namely relative draft and relative width. Compared to the experimental data, the numerical model predicts the hydrodynamics around the double-floating breakwater. The transmission coefficient decreases with increasing relative width for all relative distances [35]. Mani [36] investigated the transmission coefficients on pontoons, mats, and moored breakwaters. Murani and Mani [37] tested performance on a cage-type due to wave effects and wave-current interaction. Analysis of pontoon-type behavior experimentally, theoretically, and the dynamic response of motion, mooring force, and wave attenuation were investigated by Sannasiraj et al. [29], Duan et al. [38] determined the transmission coefficient based on the ratio of the width of the structure to the wavelength of F-type. Experimental analysis of floating breakwaters of piled and moored types with various configurations of mooring angles was investigated by Sujantoko et al. [39]. Analysis of mooring line tension on saw type [40], wave transmission on the hexagonal type [41], the effect of stability of concrete anchor block on steep-floating breakwater [42], and effect of dynamic response behavior on structure [18, 43].

In general, the floating breakwater will decrease wave energy by reflecting waves, destroying the movement of water particles, and lowering water viscosity. If an ocean wave hits the structure, the wave energy will be reflected and scattered and will cause the motion structure. This induced structural motion will generate waves, which the mooring system will limit. [40]. Based on the concept of maximum wave energy dissipation, floating breakwater research will continue to develop to produce effective and efficient performance. Some researchers have conducted studies of floating breakwaters in the porous form in various types, namely porous pontoons [44, 45], porous boxes [19, 46], porous plate [47-49], porous pipe/cylinder [50-52], and saw porous [18, 20].

The study of slope-porous shapes with various variations of slope and porosity has been carried out experimentally at the model scale of 1:20 [21, 53] in Figure 1. The floating breakwater models are moored at an angle of 45 degrees with a position of 10.2 m from wave probe 1 (wp1) with a fixed water depth of 0.75 m. The reflected waves are recorded in two wave probes, mounted 1.5m (wp2) and 1.0m (wp3) in front of the model. In contrast, the transmitted wave was measured in wp4, set at 1.0m behind the model. This research shows that the pore shape can reduce the load on the mooring rope, but the transmission becomes more significant than the impermeable shape. Vice versa, the reflection of the wave is small.

(a) Model 1

(b) Model 2

(c) Model 3

(d) Model 4

(e) Model 5

Figure 1 Floating breakwater models
Slika 1. Modeli plutajućih lukobrana

3. MATERIAL AND METHOD / *Materijal i metoda*
3.1. Computational Fluid Dynamics / *Računalni model dinamike tekućine*

This research was completed by modeling CFD (computational fluid dynamics). In this CFD modeling, the fluid flow environment is limited to specific boundary conditions to simulate the effects around the area that is the focus of the investigation. The principle of three-dimensional flow explains that the fluid flow behavior is solved by the RANS (Reynolds Averaged Navier-Stokes) equation below. The fluid flow equations for the control volume are solved on a staggered and finite difference structured grid. The computational grid is made on a three-dimensional rectangular grid. The free surface is traced by combining the VOF method with RANS. In the calculation of turbulence flow, the turbulence Renormalization-Group (RNG) is used because it has a low Reynolds number effect and is most accurate for real-world problems at best [54]. The RNG model uses an equation identical to the equation for the k-e model. This approach uses a statistical approach to derive the average equation for turbulence quantities, such as turbulent kinetic energy and dissipation rate. The RNG model generally has a broader application than the standard k-e model [55]. The RANS equation is stated as follows:

$$\frac{\partial u}{\partial t} + \frac{1}{V_F}\left[uA_x\frac{\partial u}{\partial x} + vA_yR\frac{\partial u}{\partial y} + wA_z\frac{\partial u}{\partial z}\right] - \xi\frac{A_yv^2}{xV_F} = -\frac{1}{\rho}\frac{\delta p}{\delta x} + G_x + f_x - b_x - \frac{R_{SOR}}{\rho V_F}(u - u_w - \delta_{u_s}) \tag{1}$$

$$\frac{\partial v}{\partial t} + \frac{1}{V_F}\left[uA_x\frac{\partial v}{\partial x} + vA_yR\frac{\partial v}{\partial y} + wA_z\frac{\partial v}{\partial z}\right] + \xi\frac{A_yuv}{xV_F} = -\frac{1}{\rho}\frac{\delta p}{\delta y} + G_y + f_y - b_y - \frac{R_{SOR}}{\rho V_F}(v - v_w - \delta_{v_s}) \tag{2}$$

$$\frac{\partial w}{\partial t} + \frac{1}{V_F}\left[uA_x\frac{\partial u}{\partial x} + vA_yR\frac{\partial u}{\partial y} + wA_z\frac{\partial u}{\partial z}\right] = -\frac{1}{\rho}\frac{\delta p}{\delta z} + G_z + f_z - b_z - \frac{R_{SOR}}{\rho V_F}(w - w_w - \delta_{w_s}) \tag{3}$$

Where fluid velocity on the axis (u, v, w), fractional open volume at open flow (V_F), the fractional open area of the fluid flow in the axis (A_x, A_y, A_z), acceleration due to gravity on the axis (G_x, G_y, G_z), the viscous acceleration (f_x, f_y, f_z), loss of flow in a porous medium or across a porous insulating plate (b_x, b_y, b_z), and the final term is the mass of the geometric component.

CFD is a numerical modeling method that can be used in experiments or modeling related to fluid flow. This research is modeling the floating breakwater in the wave tank. The expected output is the water level before and after being exposed to the structure. However, as needed, other outputs are also obtained in addition to the surface height value, such as water pressure conditions, wave-particle velocity, turbulence, and many more. This CFD also has several advantages. It has an easy-to-understand display in making input configurations for a model, observations of the results of running models can be seen visually in every position required, and the output is displayed in the form of images and videos.

### 3.2. Numerical Modeling / *Numeričko modeliranje*

The floating breakwater model for numerical modeling is done with SolidWorks software. Good numerical modeling results can be achieved by arranging the dimensions of the waves according to the conditions during the experiment at a water depth of 0.75 m. After modeling the wave tank, the next step is to arrange the number of meshes. The meshing used in the modeling is 0.05-0.08 m (Figure 2). The next step is to set up the physical model of CFD's

floating breakwater and mooring lines. The structure is placed facing the Xmax direction, or the positive x-axis, with the mooring rope coordinates adjusting to the slope angle of the floating breakwater (Figure 3).

The hydrostatic input properties include the fluid density of 1000 kg/m3, the gravity of 9.8 kg/m2 towards the negative z-axis, and the turbulent motion used is laminar. The boundary conditions in this modeling are as follows: a) *Waves (Wv)*. In this boundary condition, waves can enter the computational area and propagate in the expected direction to other boundary conditions. Data on the wave type, wave period, wave amplitude, and water depth are entered in this boundary condition. This boundary condition is defined on the right (XMax). b) *Symmetry* is a boundary condition with no scalar flux flow along the boundary. c) *Walls (W)*. Boundary conditions where a watertight wall surrounds the mesh tank, and d) *Outflow (O)* is a boundary condition used for the modeled wave flow to escape to prevent fluid from accumulating behind the wave tank. In this boundary condition, a wave absorber is also modeled so that no reflection occurs behind the structure. After setting the boundary conditions (Figure 4), the next step is to place the history probe by the experimental results, which retrieve water level elevation data at specific predetermined points. The type of history probe used is a fluid probe: Stationary or attached, which allows this probe to remain in position. Examples of free surface elevation results can be seen in Figures 5 and 6.
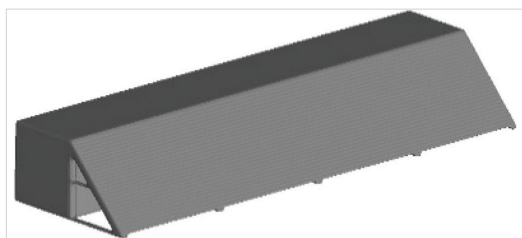
(a) porosity 0%
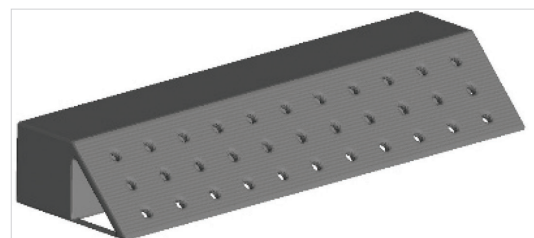
(b) porosity 5%

Figure 2 Example of 3D geometric model floating breakwaters
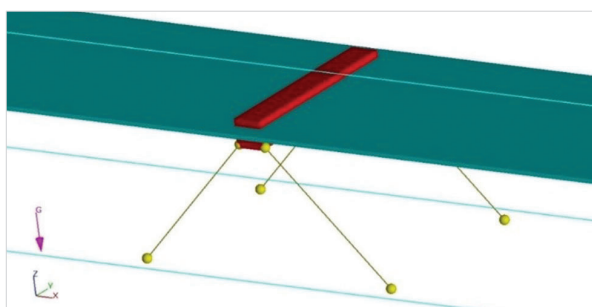*Slika 2. Primjer 3D geometričkih modela plutajućih lukobrana*

Figure 3. Modeling of the floating breakwater in a wave tank
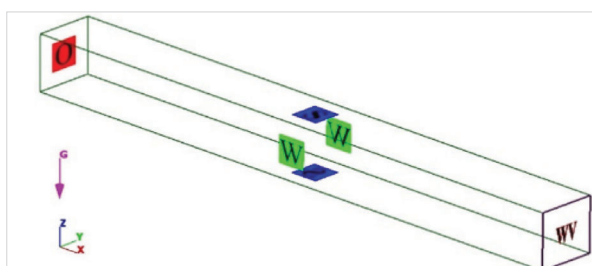*Slika 3. Modeliranje plutajućega lukobrana u tanku vala*

Figure 4 Boundary condition in domain computation
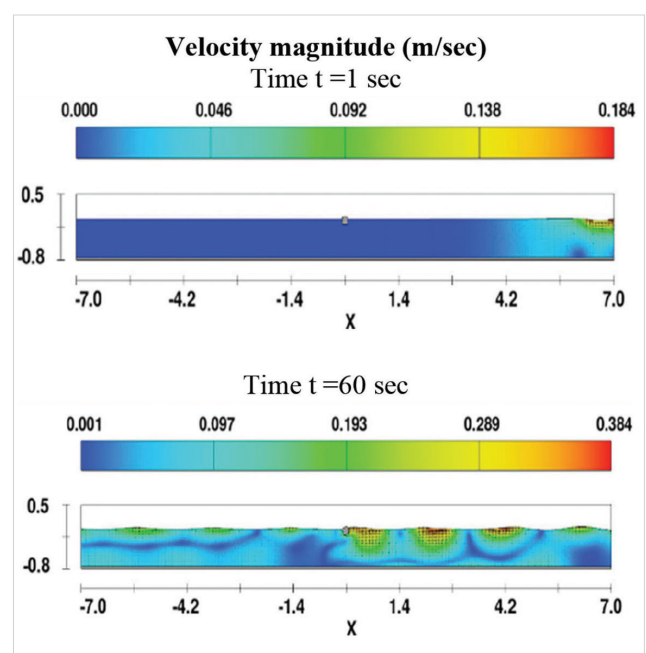*Slika 4. Rubni uvjeti u računalnoj domeni*

Figure 5 Free surface elevation contour
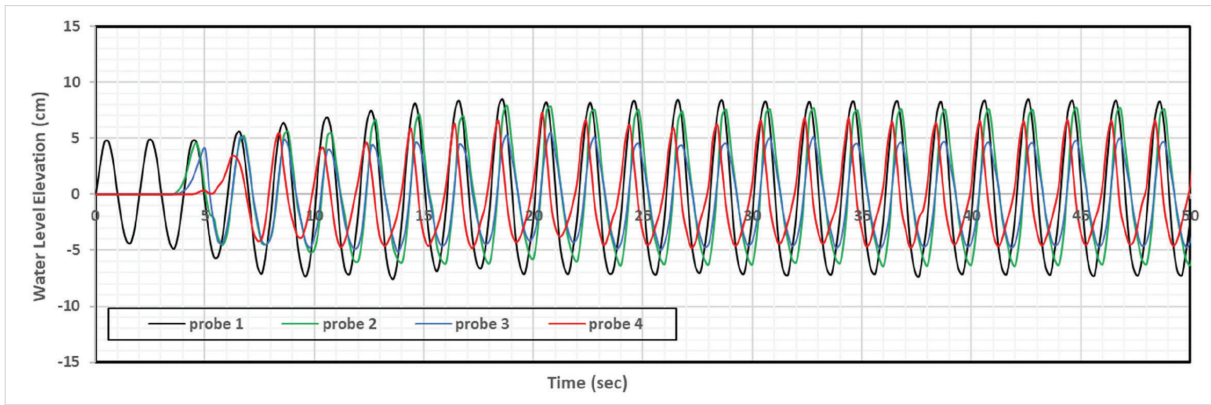*Slika 5. Kontura elevacije slobodne površine*

Figure 6 Free surface elevation profile
Slika 6. Profil elevacije slobodne površine

Details of the flow on the surface of the structure (wp5) and the pore structure (wp6) are shown in Figures 7 and 8. Generally, the flow velocity at the structure's surface is more significant than after passing through the structure. Based on this phenomenon,

Figure 7 Flow velocity vector (cm/s) around a porous-slope floating breakwater
Slika 7. Vektor tijeka brzine (cm/s) oko poroznoga kosog plutajućeg lukobrana

the pore shape is also very efficient in reducing the water content. In addition, it can absorb wave energy not entirely, so the mooring force received due to wave energy can be reduced.
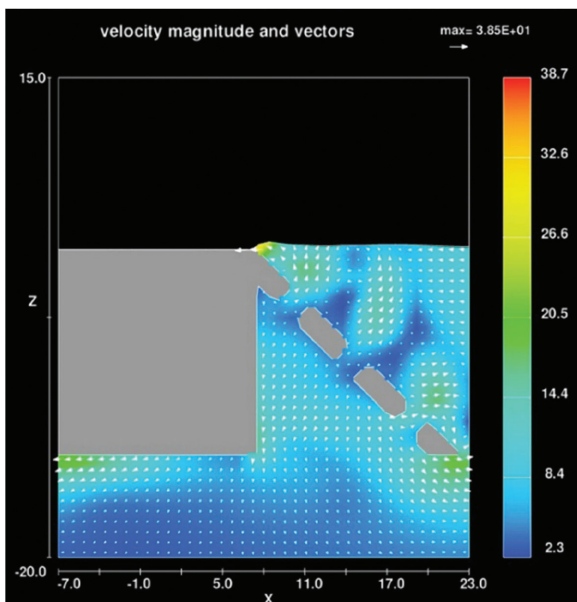
3.3. Wave Transmission and Reflection Analysis / *Analiza transmisije i refleksije vala*

The hydrodynamic performance of the floating breakwater is defined by the transmission (K_t) and reflection (K_r) coefficient. K_t is expressed as the ratio of the height of the transmission wave H_t to the incident wave H_i. When the K_t value is small, the structure can reduce the wave well. At the same time, K_r is the result of comparing the height of the reflected wave Hr with the income wave H_i. The floating structure is an effective anti-reflective structure with a low K_r value.

The incident and reflected waves due to marine structures can be determined using Goda and Suzuki methods [56]. Two wave probes record changes in water level simultaneously. This method works by separating the incoming and reflected waves to determine K_r.

3.4. Mooring Line System / *Sustav užadi za privezivanje*

The mooring system is used to hold the floating structure in place. This study used mooring ropes with a taut system (Figure 9). The taut system utilizes the mooring system's tension to withstand the structure's buoyancy so that it has a lower mooring radius. The length of the mooring line (*l*) can be determined analytically.

Motion in floating structures due to the influence of wave forces will cause tension (T) in the mooring line. The stresses on the mooring line can be divided into a) Mean tension, the tension
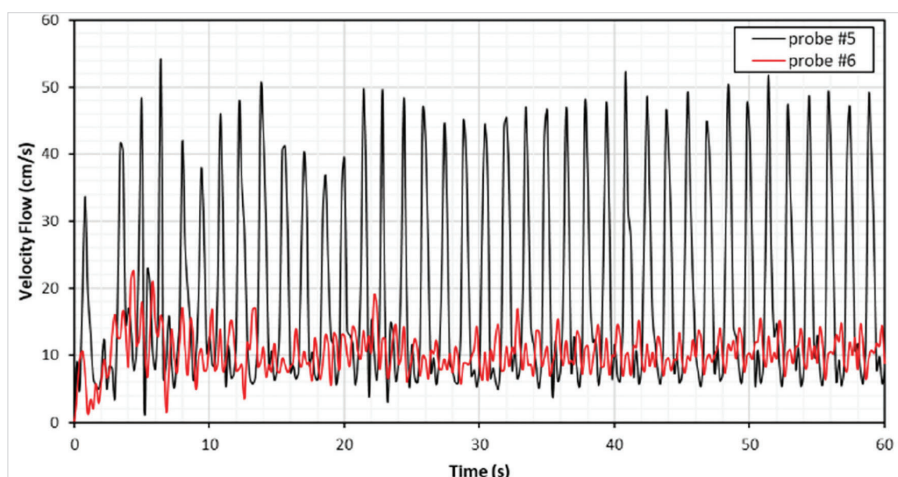

Figure 8 Flow velocity at the surface of the structure and after passing through the pores in the floating breakwater
Slika 8. Tijek brzine na površini strukture nakon prolaska porama plutajućega lukobrana

on the mooring line related to the mean offset, and b) Maximum tension. A combination of wave frequency and low-frequency tension influences the mean tension.
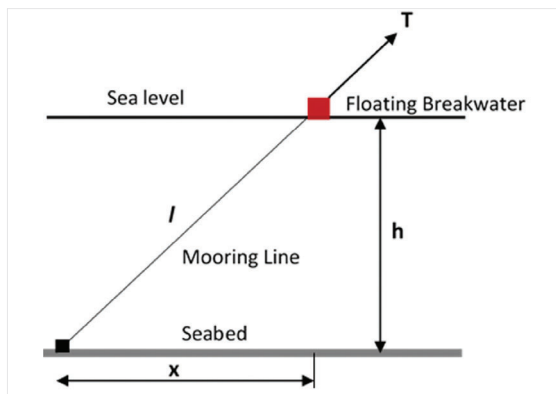

Figure 9 Configuration of mooring lines with a taut system on a floating breakwater
Slika 9. Konfiguracija užadi za privezivanje sustavom napinjanja na plutajućemu lukobranu

According to Faltinsen [57], the calculation of the maximum tension of the mooring rope can use the equation below:

$$T_{max} = T_H + w\,h \tag{4}$$

Where T_{max} maximum mooring rope tension (tonnes), T_H horizontal pre-tension (tonnes), w chain weight in water (tonnes/m), and h water depth (m).

In this study, floating breakwaters were moored with mooring lines with a configuration of 45 deg [21] [53] as the initial analysis. Furthermore, to see the mooring angle's influence on transmission and reflection coefficients, the mooring angle was varied at an angle of 30, 45, 60, and 90 deg. In this study, mooring ropes used springs to substitute the chains generally utilized in mooring techniques. The spring wire has a diameter of 2 mm, an outer diameter of 6.5 mm, a length of 820 mm, and a stiffness of 4.28 N/mm².

4. RESULTS AND DISCUSSION / *Rezultati i rasprava*
4.1. Wave Transmission Coefficient Validation / *Validacija koeficijenta transmisije vala*

The results of the transmission coefficient analysis for each model are plotted to determine the effect of the wave parameter number (H/gT²) on the transmission coefficient using a linear equation. It was found that linear variation gave the most significant R² value. Based on the data from the analysis of the transmission coefficient, it is possible to compare each model with the results of previous experimental tests [21]. The following is a comparison graph of the transmission coefficient of each model (Figure 10).
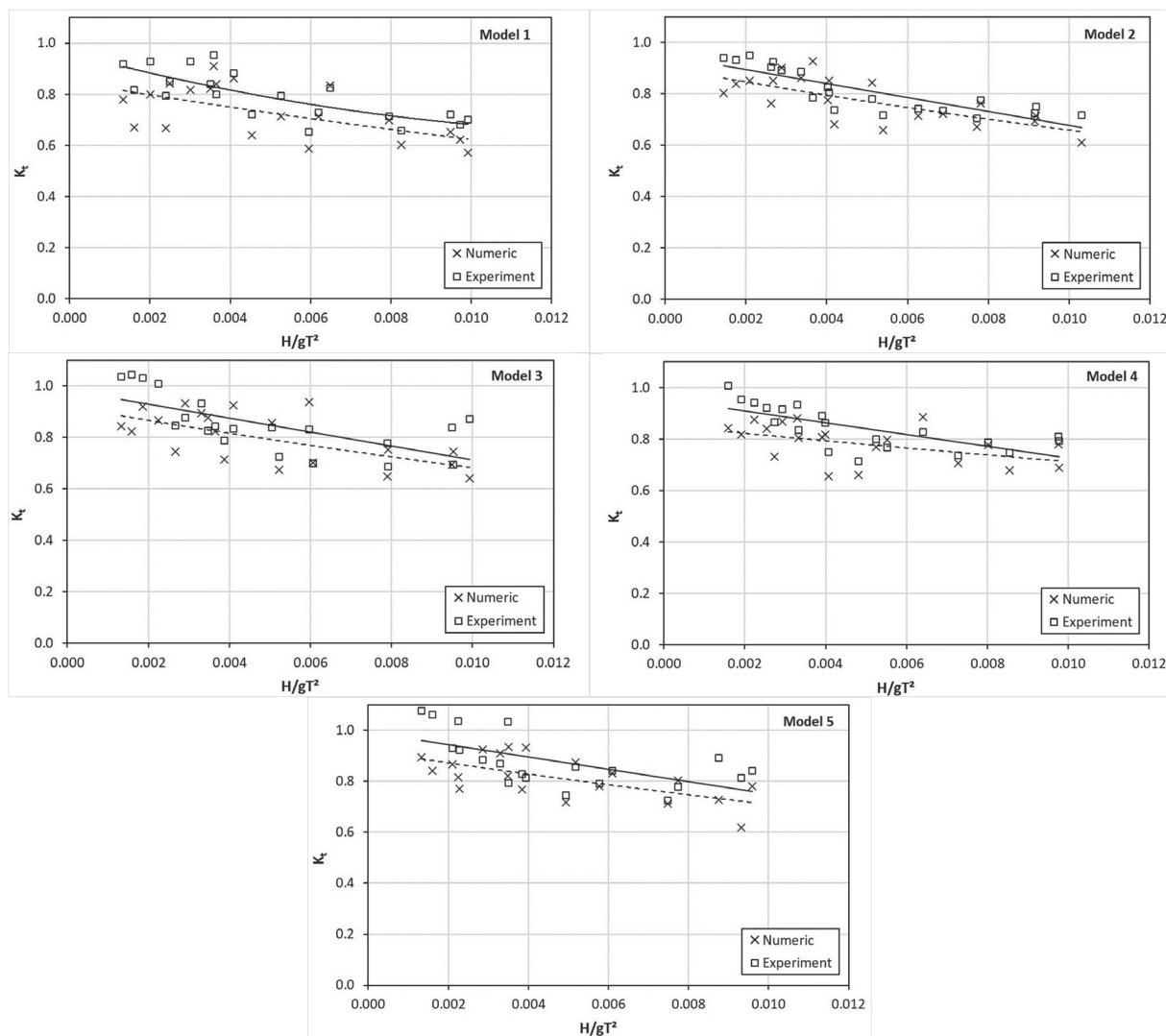

Figure 10 Comparison of transmission coefficients in models 1 to 5
Slika 10. Usporedba koeficijenata transmisije pri modelu 1 do 5

Based on the picture above, it can be shown that the trendline of numerical simulation results and experiments is relatively the same. The difference in error between the results of the numerical model and the experiment average transmission coefficient (K_t) of each model is shown in Table 2. The error values in models 1 to 5 are 7.9%, 4.54%, 5.98%, 6.97%, and 6.88%, respectively. The overall result between numerical and experimental modeling is still below 10%, so the modeling is quite good. In the results of numerical and experimental modeling, there are slight differences in values where the CFD modeling has a smaller K_t than the experimental results. Several causes exist for these differences, including human factors in the experiment; excessive surge floating breakwater motion can also increase the transmission coefficient. This excess motion can occur because of differences when modeling the floating breakwater and its mooring rope. Not all phenomena during the physical model test can be modeled numerically.

The analysis of the results of K_t shows that the gentler the slope of the floating breakwater will be, the smaller the K_t will be, and the more impermeable the slope of the structure will be, the smaller the value of K_t will be.

Table 2 Validation of wave transmission coefficient
Tablica 2. Validacija koeficijenta transmisije vala

| Model | K_t | | Error |
	Numeric	Experiment	%
Model 1	0,73	0,80	7,90
Model 2	0,77	0,81	4,54
Model 3	0,80	0,85	5,98
Model 4	0,78	0,84	6,97
Model 5	0,82	0,88	6,88

4.2. Wave Reflection Coefficient Validation / *Validacija koeficijenta refleksije vala*

The results of the analysis of the numerical model of the reflection coefficient K_r are summarized in Figure 11. Table 3 shows the average reflection coefficient error for each model. The reflection coefficient values in Models 1 to 5 are 5%, 6.79%, 10.24%, 4.07%, and 5.45%, respectively. By making comparisons based on the shape of impermeable and porous structures (see Figure 1), it can be explained that the more gentle the slope of the floating breakwater, the smaller the reflection coefficient, and conversely, the steeper the slope of the floating breakwater, the larger the reflection coefficient.
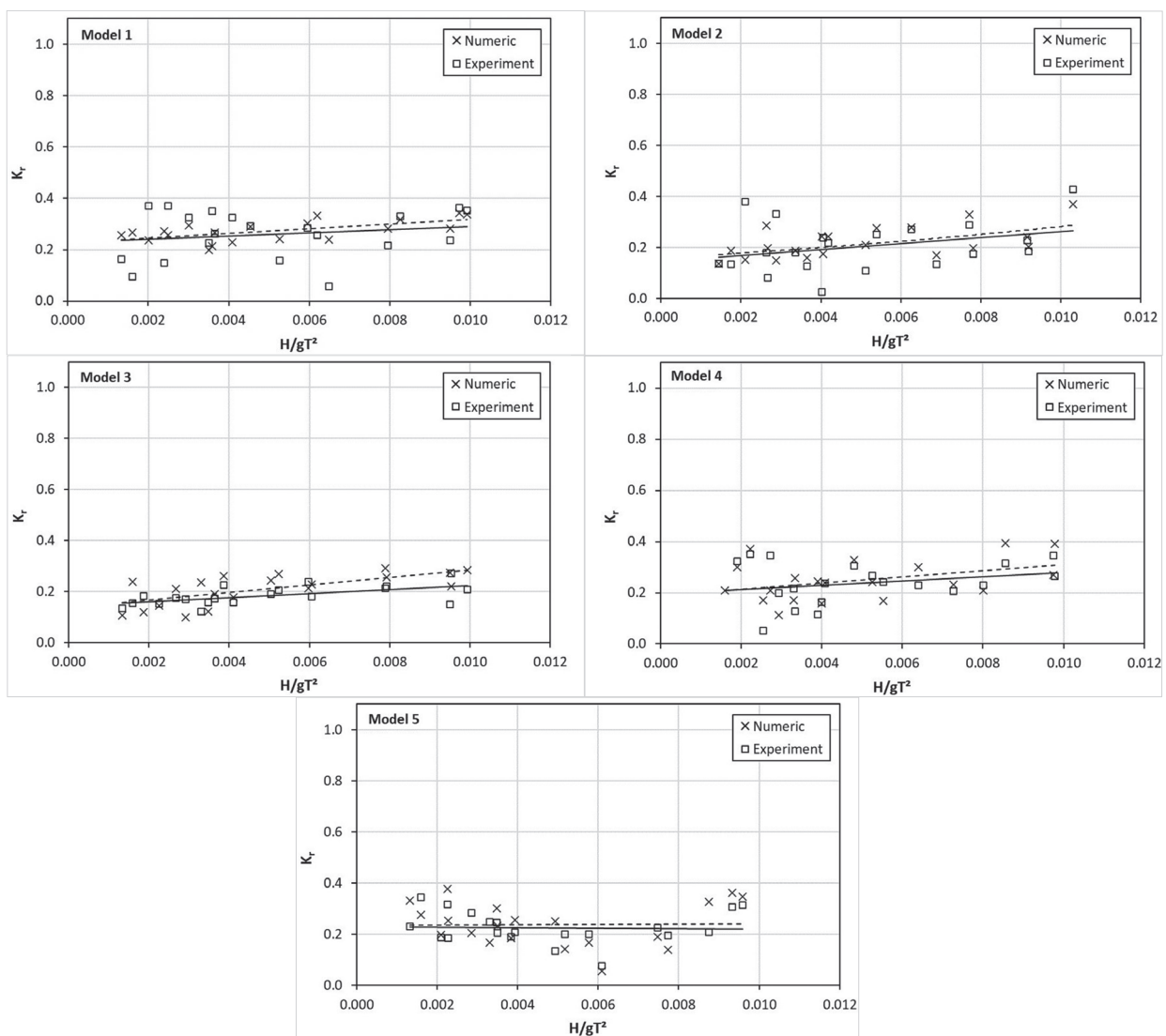

Figure 11 Comparison of reflection coefficients in models 1 to 5
Slika 11. Usporedba koeficijenata refleksije pri modelu 1 do 5

A comparison of reflection coefficients shows that the simulation and experimental results differ. This difference occurs because, during the experimental test, there was a reflection from the walls of the flume tank, which caused the water elevation read on the wave probe to rise. Based on research by Mansard and Funke [58], to get good results on the Goda and Suzuki method [56], the distance between the wave probes that record the water level elevation data due to reflections from the structure must be changed every different period. So this method does not produce the maximum reflection coefficient.

Table 3 Validation of wave reflection coefficient
Tablica 3. Validacija koeficijenta refleksije vala

Model	K_r		Error
	Numeric	Experiment	%
Model 1	0,27	0,26	5,00
Model 2	0,22	0,20	6,79
Model 3	0,21	0,18	10,24
Model 4	0,25	0,24	4,07
Model 5	0,24	0,23	5,45

4.3. Effect of Mooring Line Angle on K_t and K_r / *Efekt kuta užeta za privezivanje na K_t i K_r*

After the calibration process, the coefficients of transmission and reflection of the floating breakwater are determined using CFD simulation due to the influence of changes in the mooring rope angle. In this exploration model, model 2 is used because it is considered the most optimal in reducing waves and has the slightest error than other models. Simulations were carried out at wave periods, T=2 seconds, and wave heights H= 5cm, 7.5cm, 10cm, and 12.5cm with the configuration of the mooring rope angles of 90°, 60°, 45°, and 30°.

The simulation results of the mooring line angle on the transmission and reflection coefficients are shown in Figures 12 and 13. It can be shown that the more upright a mooring rope angle is, the higher the transmission and reflection coefficients will be. That can occur because the floating breakwater moves more freely, and there is a pulling effect from the mooring rope at an angle of 90°, which causes the transmission coefficient to be higher.
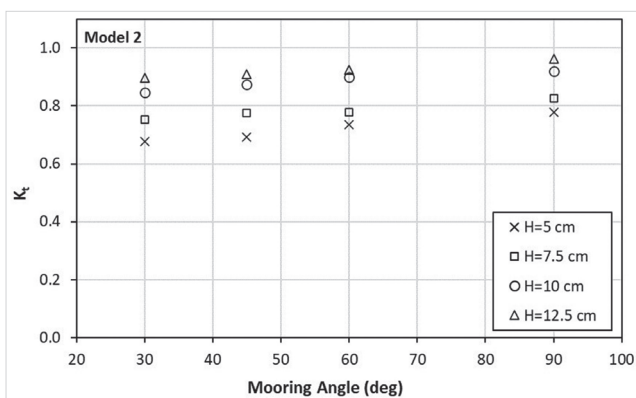

Figure 12 Comparison of K_t due to changes in mooring line angle at various wave heights in model 2
Slika 12. Usporedba K_t zbog promjena u kutu užeta za privezivanje prema različitim visinama vala na modelu 2
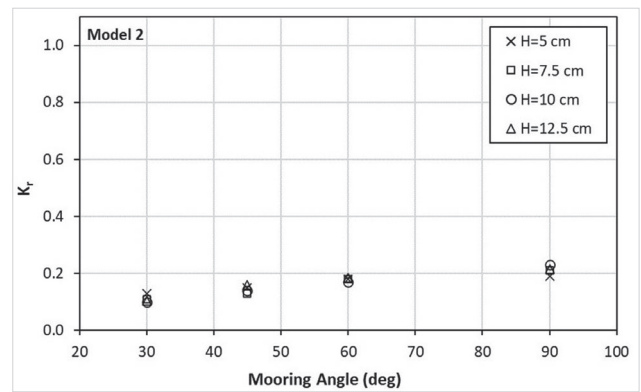

Figure 13 Comparison of K_r due to changes in mooring line angle at various wave heights in model 2
Slika 13. Usporedba K_r zbog promjena u kutu užeta za privezivanje pri različitim visinama vala pri modelu 2

4.4. Effect of Water Level Elevation on K_t and K_r / *Učinak podizanja razine mora na K_t i K_r*

The effect of changes in water level elevation (d= 85 cm, 75 cm, and 65 cm) on coefficients of transmission and reflection of the floating breakwater structure was carried out by numerical simulations in model 2. The simulations were carried out with variations in wave periods of 1.1 seconds to 2.0 seconds and wave heights of 12.5 cm. The mooring rope angle is 30° with a rope length of 150 cm.

Figures 14 and 15 show the influence of water level elevation on the transmission and reflection coefficients. The water levels of 85 cm (high tide), 75 cm (seawater line), and 65 cm (low tide) gave an average K_t of 0.86, 0.89, and 0.92. At the same time, the average K_r is 0.16, 0.13, and 0.11, respectively. The graph shows that changes in water level elevation affect the transmission and reflection coefficients. At a depth of 85 cm, it produces a minor wave transmission and has the highest wave reflection rate. This condition occurs because the length of the mooring rope is designed when the water conditions when the tide is 85cm with a mooring rope length of 150 cm. So for water levels of 75 cm and 65 cm, the mooring rope will be loose and not tense, which causes the floating breakwater to move more quickly and eliminate the function of the floating breakwater itself. The phenomenon of high and low tides must be considered by engineers when designing the structure in the coastal area.
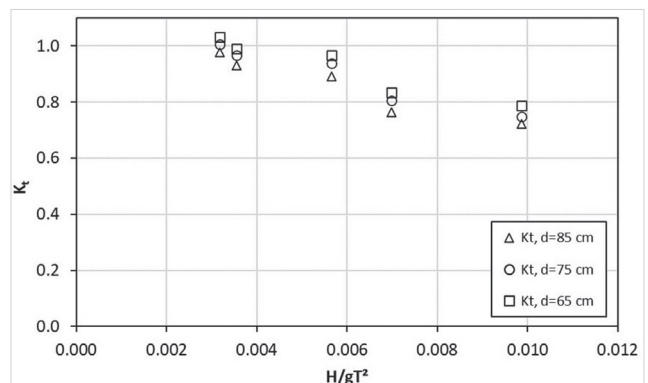

Figure 14 Comparison of K_t due to changes in water level elevation in model-2
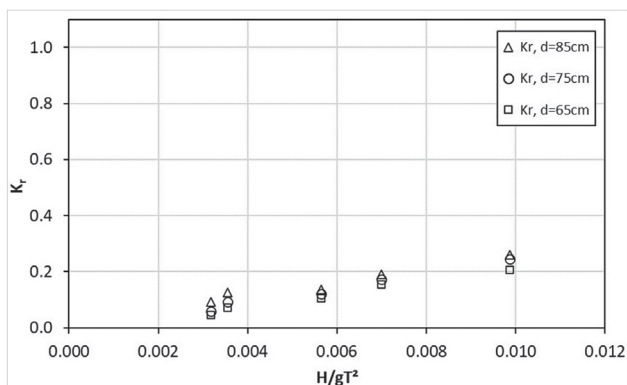*Slika 14. Usporedba K_t zbog podizanja morske razine – model 2*

Figure 15 Comparison of K_r due to changes in water level elevation in model 2

Slika 15. Usporedba K_r zbog promjena u podizanju morske razine – model 2

5. CONCLUSIONS / *Zaključci*

Numerical modeling has been carried out on the floating breakwater model with variations in height and wave period on regular waves. The model validation results between numerical and experimental showed quite good results, namely a maximum of 10% for wave transmission and reflection. Several causes for these differences include excessive surge floating breakwater motion, which can increase the transmission coefficient. This excess motion can occur because of differences when modeling the floating breakwater and its mooring rope. Besides that, there is also a wave reflection from the wall of the wave flume, causing the water elevation read by the wave probe to be high. Based on research by Mansard and Funke, to get good results on the Goda and Suzuki method, the distance between the wave probes that record the water level elevation data due to reflections from the structure must be changed every different period. So this method does not produce the maximum reflection coefficient.

Analysis of the influence of changes in the mooring line angle, the simulation is carried out at 30 deg to 90 deg and produces an average transmission coefficient of 0.79 and a reflection of 0.21. While the effect of changes in water level elevation of 0.85 m, 0.75 m, and 0.65 m gives a reasonably significant average transmission coefficient of 0.85 and a reflection of 0.13. The mooring line angle will be gentler at high tide, and the transmission and reflection coefficients will be higher. However, the mooring line will loosen at low tide, causing the structure to move more freely and eliminating the function of the floating breakwater itself. The tidal phenomenon becomes a challenge for coastal experts in designing structures to produce effective and effective and efficient hydrodynamic performance.

This slope-porous floating breakwater research needs to be studied further on other aspects, such as motion response and inter-connection module, either by experiment or numerical model.

Author Contributions: Conceptualization, S.; Methodology, S., and I. G. F.; Software, I. G. F. Formal Analysis, S. and I. G. F.; Investigation, S., E. B. D. and W.W; Resources, S. and I. G. F.; Data Curation, S. and I. G. F.; Writing - Original Draft Preparation, S. and I. G. F.; Writing - Review and Editing, S.; Visualization, S. and I. G. F; Supervision, E. B. D. and W. W.; Project Administration, S.; Funding Acquisition, S.

REFERENCES / *Literatura*

[1] Mahmud, M., Sujantoko & Prasetyo, M. A. (2022). Empowerment and Optimization of Kenjeran Beach Tourism Potential, Surabaya-East Java. *International Review of Civil on Engineering (IRECE)*, 13(4), 246-254. https://doi.org/10.15866/irece.v13i4.20659

[2] Mahmud, M., Garang, I. J., Ikhwani, H. & Sujantoko (2022). Analysis and Maximize the Ecotourism Potential of the Wonorejo Mangrove in East Surabaya. *International Journal on Engineering Applications (IREA)*, 10(2), 158-166. https://doi.org/10.15866 /irea.v10i2.21158

[3] Armono, H. D., Sujantoko, Hidayah, Z. & Nuzula, N. I. (2021). Hydro-Oceanographic Mapping to Support Coastal Eco-Tourism Activities in Bawean Island, East Java. *Sustainable Islands Development Initiatives - International Conference*, Vol. September 2019, A39-A52. https://doi.org/10.1088/1755-1315/649/1/012036

[4] Mustain, M. & Sujantoko (2023). Spiral Analysis of Vertical Currents in Lamong Bay. *The 7th International Conference on Marine Technology (SENTA)*, October 2022.

[5] Mustain, M. & Sujantoko (2022). Simple Analysis of the Determination of Tidal Types of Seawater: a Case Ctudy in Lamong Bay Waters, East Java, 2021. *IEEE Ocean Engineering Technology and Innovation Conference: Ocean Observation, Technology, and Innovation in Support of Ocean Decade of Science (OETIC)*, 13-17. https://doi.org/ 10.1109/OETIC53770.2021.9733727

[6] Armono, H. D., Winarto, A., Sujantoko & Suastika, I. K. (2021). A Laboratory Study on Wave Transmission over the Hexagonal Artificial Reef. *IOP Conference Series: Earth and Environmental Science*, 799(1), 1-9. https://doi.org/10.1088/1755-1315/799 /1/012011

[7] CERC (1984). Shore Protection Manual. Coastal Engineering Research Centre, Department of the Army Waterways Experiment Station, US Army Corps of Engineers, Washington.

[8] Allsop, N. W. H. & Hettiarachchi, S. S. L. (1989). Reflections from Coastal Structures. *Coastal Engineering*, 782-794. https://doi.org/10.1061/9780872626874.059

[9] Muttray, M., Reedijk, B. & Klabbers, M. (2005). Development and Application of an Innovative Breakwater Armour unit. *1st International Conference On Coastal Zone Management and Engineering, in The Middle East*. Retrieved from: https://www.yumpu.com/en/document/read/41908845/development-of-an-innovative-breakwater-armor-unit

[10] Zanuttigh, B. & van der Meer, J. W. (2008). Wave Reflection from Coastal Structures in Design Conditions. *Coastal Engineering*, 55(10), 771-779. https://doi.org/10.1016/ j.coastaleng.2008.02.009

[11] Pratola, L., Rinaldi, A., Molfetta, M. G., Bruno, M. F., Pasquali, D., Dentale, F. & Mossa, M. (2021). Investigation on the Reflection Coefficient for Seawalls Protected by a Rubble Mound Structure. *Journal of Marine Science and Engineering*, 9(937). https://doi.org /10.3390/jmse9090937

[12] Fousert, M. W. (2007). *Floating Breakwater: A Theoretical Study of a Dynamic Wave Attenuating System*. Master thesis, The Delft University of Technology, Faculty of Civil Engineering and Geosciences. Retrieved from: https://repository.tudelft.nl/islandora /object/uuid%3A87d7e889-8aaf-410b-9502-495412c59308

[13] Van der Meer, J. W. & Pilarczyk, K. W. (1984). Stability of Rubble Mound Slopes under Random Wave Attack. *Coastal Engineering*, 1(1). https://doi.org/10.9753/icce.v19.176

[14] Armono, H. D., Bromo, B. H., Sholihin & Sujantoko (2022). Numerical Study of Bamboo Breakwater for Wave Reduction. *Fluids*, 7(1), 14. https://doi.org/10.3390 /fluids7010014

[15] McCartney, B. L. (1985). Floating Breakwater Design. *Journal of Waterway, Port, Coastal and Ocean Engineering*, 111(2), 304-318. https://doi.org/10.1061/(ASCE)0733-950X(1985)111:2(304)

[16] Morey, B. J. (1998). Floating Breakwaters Predicting Their Performance. Master thesis, Memorial University of Newfoundland, Canada. Retrieved from: https://research.library.mun.ca /5383/2/Morey_BradleyJ.pdf

[17] Hales, L. Z. (1981). Floating Breakwater: State of the Art Literature Review. Technical Report No. 81-1. U. S. Army Coastal Engineering Research Center, Fort Belvoir. Retrieved from: https://apps.dtic.mil/sti/citations/ADA110692. https://doi.org/10.5962/bhl.title.47174

[18] Sujantoko, Djatmiko, E. B., Wardhana, W., Armono, H. D. & Wahyudi (2019). Dynamic Behavior Analysis of Porous Saw Floating Breakwater under Regular Waves. *Proceeding of The 7th International Seminars on Ocean and Coastal Engineering, Environmental and Natural Disaster Management*, Surabaya, Indonesia, Nov 6-7, 236-241. https://doi.org/ 10.5220/0010119102120217. https://doi.org/10.5220/0010119102360241

[19] Zheng, Y. N., Liu, X. M., Chen, C. P., Jiang, Y. P. & Zhang, C. W. (2018). Experimental Study on the Wave Dissipation Performance and Mooring Force of Porous Floating Breakwater. *International Conference on Civil and Hydraulic Engineering (IConCHE)*, IOP Conf. Series: Earth and Environmental Science 189. https://doi.org/10.1088/1755-1315/189/2/022058

[20] Sujantoko, Djatmiko, E. B., Wardhana, W., Armono, H. D., Sholihin & Ali, M. F. (2019). Experimental Study on the Effect of Mooring Angle on Mooring Tension of Porous Saw type Floating Breakwater. *Proceeding of The 7th International Seminars on Ocean and Coastal Engineering, Environmental and Natural Disaster Management,* Surabaya, Indonesia, Nov 6-7, 94-99. https://doi.org/10.5220/0010057000940099

[21] Sujantoko, Djatmiko, E. B. & Wardhana, W. (2022). Experimental Investigation of the Performance of Porous-Slope Floating Breakwater. *International Journal on Engineering and Applications,* 10(2), 149-157. https://doi.org/10.15866/irea.v10i2. 21350

[22] Nece, R. E. & dan Richey, E. P. (1972). Wave Transmission Tests of Floating Breakwater for Oak Harbour. Water Resources Series Tech. Report 32, Department of Civil and Environment Engineering, University of Washington. https://www.ce.washington.edu/sites/cee/files/pdfs/research/hydrology/water-resources/WRS032.pdf

[23] Blumberg, G. & Cox, R. (1988). Floating Breakwater Physical Model Testing for Marina Applications. Bulletin 63, PIANC-AIPCN.

[24] Neelamani, S. & Rajendran, R. (2002). Wave Interaction with T-type Breakwaters. *Ocean Engineering*, 29(2), 151-175. https://doi.org/10.1016/S0029-8018(00)00060-3

[25] Neelamani, S. & Rajendran, R. (2002). Wave Interaction with -type Breakwaters. *Ocean Engineering* 29(5), 561-589. https://doi.org/10.1016/S0029-8018(01)00030-0

[26] Dong, G. H., Zheng, Y. N., Li, Y. C., Teng, B., Guan, C. T. & dan Lin, D. F. (2008). Experiments on Wave Transmission Coefficients of Floating Breakwaters. *Ocean Engineering*, 35(8-9), 931-938. https://doi.org/ 10.1016/j.oceaneng.2008.01.010

[27] Koutandos, E., Prinos, P. & Gironella, X. (2005). Floating Breakwaters under Regular and Irregular Wave Forcing: Reflection and Transmission Characteristics. *Journal of Hydraulic Research,* 43(2), 174-188. https://doi.org/10.1080/00221686.2005.9641234

[28] Fugazza, M. & Natale, L. (1988). Energy Losses and Floating Breakwater Response. *Journal of Waterway, Port, Coastal and Ocean Engineering,* 114(2), 191-205. https://doi.org/10.1061/(ASCE)0733-950X(1988)114:2(191)

[29] Sannasiraj, S., Sundar, V. & Sundaravadivelu, R. (1998). Mooring Forces and Motion Responses of Pontoon-type Floating Breakwaters. *Ocean Engineering,* 25(1), 27-48. https://doi.org/10.1016/S0029-8018(96)00044-3

[30] Rahman, M. A., Mizutani, N. & Kawasaki, K. (2006). Numerical Modeling of Dynamic Responses and Mooring Forces of the Submerged Floating Breakwater. *Coastal Engineering,* 53(10), 799-815. https://doi.org/10.1016/j.coastaleng.2006.04.001

[31] Gesraha, M. R. (2006). Analysis of Π-Shaped Floating Breakwater in Oblique Waves. *Applied Ocean Research,* 28(5), 327-338. https://doi.org/10.1016/j.apor.2007.01.002

[32] Cox, R., Coghlan, I. & Kerry, C. (2007). Floating Breakwater Performance in Irregular Waves with Particular Emphasis on Wave Transmission and Reflection, Energy Dissipation, Motion, and Restraining Forces. *International Conference on Coastal Structures*, 1, 351-362. https://doi.org/10.1142/9789814282024_0032

[33] Ruol, P. & Martinelli, L. (2007). Wave Flume Investigation on Different Mooring Systems for Floating Breakwaters. *International Conference on Coastal Structures*, 1, 327-338. https://doi.org/10.1142/9789814282024_0030

[34] Martinelli, L., Ruol, P. & Zanuttigh, B. (2008). Wave Basin Experiments on Floating Breakwaters with Different Layouts. *Applied Ocean Research,* 30(3), 199-207. https://doi.org/10.1016/j.apor.2008.09.002

[35] Koftis, T. & Prinos, P. (2005). 2D-V Hydrodynamics of Double Floating Breakwaters. *Fifth International Conference on Coastal Dynamics,* April 4-8, Barcelona, Spain. https://doi.org/10.1061/40855(214)118

[36] Mani, J. S. (1991). Design of Y-frame Floating Breakwater. *Journal of Waterway, Port, Coastal and Ocean Engineering,* 117(2), 105-119. https://doi.org/ 10.1061/(ASCE) 0733-950X(1991)117:2(105)

[37] Murali, K. & Mani, J. S. (1997). Performance of Cage Floating Breakwater. *Journal of Waterway, Port, Coastal and Ocean Engineering*, 123(4), 172-179. https://doi.org/ 10.1061/(ASCE)0733-950X(1997)123:4(172)

[38] Duan, W., Xu, S., Xu, Q., Ertekin, R. C. & Ma, S. (2017). Performance of an F-type Floating Breakwater: A Numerical and Experimental Study. *Journal Engineering for the Maritime Environment,* 231(2), 583-599. https://doi.org/10.1177/1475090216673461

[39] Sujantoko, Wardhana, W., Djatmiko, E. B., Armono, H. D., Putro, W. S. & Almuzaki, R. H. (2021). Study of Wave Characteristics of the Floating Breakwater for Piling and Tethered type. *Journal of Hydraulic Engineering (Indonesian)*, 12(1), 39-51. https://doi.org/10.32679/jth.v12i1.650.

[40] Sujantoko, Djatmiko, E. B., Wardhana, W. & Hidayatullah, A. (2021). Analysis of Mooring Tension on the Saw-type Floating Breakwater with Physical Modeling. J*ournal of Civil Engineering (Indonesian)*, 28(3), 289-300. https://doi.org/10.5614/jts.2021. 28.3.6

[41] Sujantoko, Armono, H. D., Wisnu, W. & Kurniawan, D. (2021). Wave Transmission Analysis on Hexagonal shape Floating Breakwater. I*nternational Journal of Offshore and Coastal Engineering (IJOCE),* 4(4), 171-176. http://dx.doi.org/10.12962/j2580-0914.v4i4.10934

[42] Sujantoko, Armono, H. D., Djatmiko, E. B. & Putra, R. D. (2022). Stability Analysis of Concrete Block Anchor on Steep-Slope Floating Breakwater. *Fluids*, 7(8), 259. https://doi.org/10.3390/fluids7080259.

[43] Djatmiko, E. B., Syahroni, N., Sujantoko, Supomo, H. & Nugroho, S. (2019). Evaluation of Articulated Tower-Ocean Wave Energy Converter (AT-OWEC)-Part I: the Dynamic Behaviour under Wave Excitation. *International Review of Mechanical Engineering (IREME)*, 13(10), 568-575. https://doi.org/10.15866/ireme.v13i10.16398

[44] Williams, A. N. & Li, W. (1998). Wave Interaction with a Semi-Porous Cylindrical Breakwater Mounted on a Storage Tank. *Ocean Engineering*, 25, 95-219. https://doi.org/10.1016/S0029-8018(97)00006-1

[45] Wang, H. Y. & Sun, Z. C. (2010). Experimental Study of a Porous Floating Breakwater. *Ocean Engineering*, 37, 520-527. https://doi.org/10.1016/j.oceaneng.2009.12.005

[46] Stainissie, M. & Drimer, N. (2003). On a Freely Floating Porous Box in Shallow Water Waves. *Applied Ocean Research,* 25, 263-268. https://doi.org/10.1016/j.apor. 2003.12.001

[47] Chwang, A. T. & dan Dong, Z. N. (1984). Wave-Trapping Due to a Porous Plate. *Proceedings Fifteenth ONR Symposium of Naval Hydrodynamics,* 407-414.

[48] Cho, I.-H. (2016). Transmission Coefficients of a Floating Rectangular Breakwater with Porous Side Plates. *International Journal of Naval Architecture and Ocean Engineering,* 8, 53-65. https://doi.org/10.1016/j.ijnaoe.2015.10.002

[49] Fang, Z., Xiao, L., Kou, Y. & dan Li, J. (2018). Experimental Study of the Wave-Dissipating Performance of a Four-Layer Horizontal Porous-Plate Breakwater. *Ocean Engineering,* 151, 222-233. https://doi.org/10.1016/j.oceaneng.2018.01.041

[50] Williams, A. N., Li, W. & Wang, K. H. (2000). Water Wave Interaction with a Floating Porous Cylinder. *Ocean Engineering,* 27, 1-28. https://doi.org/10.1016/S0029-8018 (98)00078-X

[51] Zhao, F., Bao, W., Kinoshita, T. & Itakura, H. (2010). Interaction of Waves and a Porous Cylinder with an Inner Horizontal Porous Plate. *Applied Ocean Research,* 32, 252-259. https://doi.org/10.1016/j.apor.2009.11.003

[52] Shih, R.-S. (2012). Experimental Study on the Performance Characteristics of Porous Perpendicular Pipe Breakwaters. *Ocean Engineering*, 50, 53-62. https://doi.org/ 10.1016/j.oceaneng.2012.05.010

[53] Sujantoko, Djatmiko, E. B. & Wardhana, W. (2022). Experimental Study on Mooring Tension of Porous-Slope type Floating Breakwater. *International Journal on Engineering and Applications,* 10, 5. https://doi.org/10.15866/irea.v10i5.22233

[54] Koutsourakis, N., Bartzis, J. G. & Markatos, N. C. (2012). Evaluation of Reynolds Stress, k- and RNG k- Turbulence Models in Street Canyon Flows using Various Experimental Datasets. *Environmental Fluid Mechanics*, 12, 379-403. https://doi.org/10.1007/si0652-012-9240-9

[55] Flow Science (2014). FLOW-3D Documentation Release 11.0.0. Flow Science, Inc. https://www.flow3d.com

[56] Goda, Y. & Suzuki, Y. (1976). Estimation of the Incident and Reflected Waves in Random Wave Experiments. P*roceedings of the 15th International Conference on Coastal Engineering*, ASCE, Honolulu, Hawai, USA, 828-845. https://doi.org/10.1061 /9780872620834.048. https://doi.org/10.9753/icce.v15.47

[57] Faltinsen, O. M. (1990). Sea Loads on Ships and Offshore Structures. United Kingdom: Cambridge University Press.

[58] Mansard, E. P. D. & Funke, E. R. (1980). The Measurement of Incident and Reflected Spectra using a Least Squares Method. *Coastal Engineering*, 154-172. https://repository.tudelft.nl/islandora/object/uuid%3A840a64af-b113-4372-8f91-47b4d7a3cc78. https://doi.org/10.1061/9780872622647.008. https://doi.org/10.9753/icce.v17.8